Molecular Structure of 2,4-Ethanotetraborane(10), $B_4H_8(CH_2)_2$, As Determined by Gas-Phase Electron Diffraction and *ab Initio* Computations†

Drahomír Hnyk,‡ Paul T. Brain, David W. H. Rankin,* and Heather E. Robertson

Department of Chemistry, University of Edinburgh, West Mains Road, Edinburgh, EH9 3JJ, U.K.

Robert Greatrex, Norman N. Greenwood, and Martin Kirk

School of Chemistry, University of Leeds, Leeds, LS2 9JT, U.K.

Michael Bühl and Paul von Ragué Schleyer

Institut für Organische Chemie der Universität Erlangen-Nürnberg, Henkestrasse 24, D-91054 Erlangen, Germany

Received November 2, 1993®

The structure of gaseous 2,4-ethanotetraborane(10), $B_4H_8(CH_2)_2$, more commonly referred to as dimethylenetetraborane, has been determined by electron diffraction and *ab initio* computations. The results confirm that the molecule consists of a tetraborane(10) cage substituted at the "wing" boron atoms, B(2) and B(4), by a bridging "ethene", C_2H_4, moiety. The molecular symmetry is C_{2v}, the conformation about the C–C bond being eclipsed. Salient structural parameters (r_a) of the experimental geometry are r[B(1)–B(2)](hinge–wing) = 189.5(3), r[B(1)–B(3)](hinge–hinge) = 172.9(17), r(B–C) = 159.8(3), and r(C–C) = 156.8 (fixed) pm; B(1)B(2)B(3) = 54.2(5)°, and the dihedral ("butterfly") angle between the planes B(1)B(2)B(3) and B(1)B(4)B(3) is 100.8(2)°. These values agree well with the *ab initio* (MP2/6-31G*) optimized molecular geometry and are supported by comparison of the calculated (IGLO) ^{1}H, ^{11}B, and ^{13}C NMR chemical shifts, using both the MP2/6-31G* and GED geometries, with the experimental NMR data.

Introduction

The compound 2,4-ethanotetraborane(10), $B_4H_8(CH_2)_2$ (henceforth referred to as dimethylenetetraborane, its more common name), was first synthesized in 1960 by the hot–cold reaction of tetraborane(10), B_4H_{10}, with ethene.[1] On the basis of the infrared and NMR studies,[1-4] a cyclic bridge structure, in which the carbon atoms of the C_2H_4 moiety are bonded to the "wing" boron atoms, B(2) and B(4) of the "butterfly"-shaped B_4H_8 unit, has been proposed. Thus, although the compound is formally classified as an *hypho*-dicarbaborane (*i.e.* $4n + 8 = 32$ valence electrons),[5] it is more usually regarded as an ethene adduct of tetraborane(8) or as an alkyl derivative of tetraborane(10).[1-3] In the context of the former, it represents the only known example of a compound in which the reactive intermediate $\{B_4H_8\}$ is stabilized by a bridging ligand.

The molecular structures of B_4H_{10} and the isomers of B_4H_8-(CO) have been determined by electron diffraction in the gas phase[6,7] and by *ab initio* computations;[8] a single-crystal X-ray diffraction study of $B_4H_8{\cdot}PF_2(NMe_2)$ has been reported.[9] To gain further insight into the structural and electronic properties of this series of compounds, we now present the results of an electron-diffraction (GED) and *ab initio* study of gaseous dimethylenetetraborane.

It has recently become possible to predict the structures of relatively large boranes using the combined *ab initio*/IGLO/NMR method.[8,10-13] In this approach, various structures derived from experiment and from *ab initio* geometry optimizations are assessed by means of IGLO (individual gauge for localized orbitals)[12] NMR calculations. The ^{11}B chemical shifts obtained by this method for various geometries are compared with the experimental chemical shifts. Using geometries optimized at electron-correlated levels of theory (*e.g.* MP2/6-31G*, *i.e.* with a basis set including polarization functions), the agreement between experimental and IGLO ^{11}B chemical shifts has been found to be consistently good.[8a]

* Author to whom correspondence should be addressed.

† A preliminary version of this work was presented at the IMEBORON VIII meeting, Knoxville, TN, July, 1993.

‡ On leave from the Institute of Inorganic Chemistry of the Academy of Sciences of the Czech Republic, 250 68 Řež near Prague, Czech Republic.

® Abstract published in *Advance ACS Abstracts*, April 15, 1994.

(1) Harrison, B. C.; Solomon, I. J.; Hites, R. D.; Klein, M. J. *J. Inorg. Nucl. Chem.* **1960**, *14*, 195.
(2) Shapiro, I.; Williams, R. E.; Gibbins, S. G. *J. Phys. Chem.* **1961**, *65*, 1061.
(3) Onak, T.; Gross, K.; Tse, J.; Howard, J. *J. Chem. Soc., Dalton Trans.* **1973**, 2633.
(4) Kirk, M.; Ph.D. Thesis, University of Leeds, 1991.
(5) Williams, R. E.; *Adv. Inorg. Chem. Radiochem.* **1976**, *18*, 67. Wade, K. *Adv. Inorg. Chem. Radiochem.* **1976**, *18*, 1.
(6) Dain, C. J.; Downs, A. J.; Laurenson, G. S.; Rankin, D. W. H. *J. Chem. Soc., Dalton Trans.* **1981**, 472.
(7) Cranson, S. J.; Davies, P. M.; Greatrex, R.; Rankin, D. W. H.; Robertson, H. E. *J. Chem. Soc., Dalton Trans.* **1990**, 101.
(8) (a) Bühl, M.; Schleyer, P. v. R. *J. Am. Chem. Soc.* **1992**, *114*, 477. (b) Bühl, M.; Schleyer, P. v. R. *Struct. Chem.* **1993**, *4*, 1. (c) Bühl, M.; Schleyer, P. v. R. In *Electron Deficient Boron and Carbon Clusters*; Olah, G. A., Wade, K., Williams, R. E., Eds.; Wiley: New York, 1991; Chapter 4, p 113.
(9) La Prade, M. D.; Nordman, C. E. *Inorg. Chem.* **1969**, *8*, 1669.
(10) (a) Schleyer, P. v. R.; Bühl, M.; Fleischer, U.; Koch, W. *Inorg. Chem.* **1990**, *29*, 153. (b) Bühl, M.; Schleyer, P. v. R. *Angew. Chem., Int. Ed. Engl.* **1990**, *29*, 886.
(11) For other examples, see: (a) Hnyk, D.; Vajda, E.; Bühl, M.; Schleyer, P. v. R. *Inorg. Chem.* **1992**, *31*, 2464. (b) Mebel, A. M.; Charkin, O. P.; Bühl, M.; Schleyer, P. v. R. *Inorg. Chem.* **1993**, *32*, 463. (c) Onak, T.; Tseng, J.; Diaz, M.; Tran, D.; Arias, J.; Herrera, S.; Brown, D. *Inorg. Chem.* **1993**, *32*, 487.
(12) (a) Kutzelnigg, W. *Isr. J. Chem.* **1980**, *19*, 193. (b) Schindler, M.; Kutzelnigg, W. *J. Chem. Phys.* **1982**, *76*, 1919. (c) Review: Kutzelnigg, W.; Fleischer, U.; Schindler, M. In *NMR, Basic Principles and Progress*; Springer Verlag: Berlin, 1990; Vol. 23, p 165.
(13) Brain, P. T.; Hnyk, D.; Rankin, D. W. H.; Bühl, M.; Schleyer, P. v. R. *Polyhedron*, in press.

0020-1669/94/1333-2572$04.50/0

Table 1. Nozzle-to-Plate Distances, Weighting Functions, Correlation Parameters, Scale Factors, and Electron Wavelengths

molecule	Nozzle-to-plate dist/mm	Δs/nm^{-1}	s_{min}/nm^{-1}	sw_1/nm^{-1}	sw_2/nm^{-1}	s_{max}/nm^{-1}	correln param	scale factor, k[a]	electron wavelength[b]/pm
$B_4H_8(CH_2)_2$	286.12	2	20	40	122	144	0.483	0.760(21)	5.645
	128.22	4	60	80	284	336	−0.200	0.771(25)	5.644

[a] Figures in parentheses are the estimated standard deviations. [b] Determined by reference to the scattering pattern of benzene vapor.

In the electron-diffraction analysis, the parameters defining the structures of boranes, especially those for the boron framework, are often subject to significant correlation.[13] Moreover, it is possible that several geometries will fit the electron-scattering data more or less equally well and additional information (*e.g.* spectroscopic or theoretical) is required to decide which of the options is correct.[14] The electron-scattering pattern of $B_4H_8(CH_2)_2$ has been analyzed and the refined structure is found to be in good agreement with the geometry proposed by the *ab initio* study. The accuracy of the structure is further substantiated by *ab initio* energy and ^{1}H, ^{11}B, and ^{13}C chemical shift calculations.

Experimental Section

Synthesis. Dimethylenetetraborane was prepared by the hot-cold reaction of tetraborane(10), B_4H_{10}, and ethene as described by Harrison *et al.*[1] and purified by low-temperature fractional distillation. The purity of the compound was checked by reference (i) to its vapor pressure at 273 K (measured as 14 mm Hg, literature value 13.9 mm Hg[2]), (ii) to the ^{1}H and ^{11}B NMR spectra of a [$^2H_3$] chloroform solution,[2,3] and (iii) to the mass spectrum of the vapor.[2]

Electron-Diffraction Measurements. Electron-scattering intensities were recorded on Kodak Electron Image plates using the Edinburgh gas-diffraction apparatus operating at *ca.* 44.5 kV (electron wavelength *ca.* 5.7 pm).[15] Nozzle-to-plate distances were *ca.* 128 and 286 mm, yielding data in the s range 20–336 nm^{-1}; three usable plates were obtained at each distance. The sample and nozzle were held at *ca.* 291 K during the exposure periods.

The scattering patterns of benzene were also recorded for the purpose of calibration; these were analyzed in exactly the same way as those of the tetraborane(10) derivative so as to minimize systematic errors in the wavelengths and camera distances. Nozzle-to-plate distances, weighting functions used to set up the off-diagonal weight matrix, correlation parameters, final scale factors, and electron wavelengths for the measurements are collected together in Table 1.

The electron-scattering patterns were converted into digital form using a computer-controlled Joyce-Loebl MDM6 microdensitometer with a scanning program described elsewhere.[16] The programs used for data reduction[16] and least-squares refinement[17] have been described previously; the complex scattering factors employed were those listed by Fink and Ross.[18]

Theoretical Calculations. *Ab initio* computations employed standard procedures and basis sets[19] using the CADPAC and Gaussian92 programs.[20] NMR chemical shifts have been calculated using the IGLO method[12] employing a Huzinaga basis set[21] of double-ζ (DZ) and II′ quality;[12c] the latter is of triple-ζ plus polarization (TZP) quality for B and C and employs a DZ basis for H. The theoretical chemical shifts have been referenced to $BF_3{\cdot}OEt_2$ (^{11}B)[8a] and Me_4Si (^{13}C and ^{1}H)[12c] and are given in the notation "level of the chemical shift calculation//geometry employed". In addition, chemical shifts have been calculated at a correlated level of theory employing the GIAO-MP2 method[25] with TZP′

Table 2. Structural Parameters for $B_4H_8(CH_2)_2$ (Distances in pm, Angles in deg)[a,b]

param		
p_1	r[B(1)–B(2)]	189.5(3)
p_2	r[B(2)–C(5)]	159.8(3)
p_3	r[C(5)–C(6)]	156.8(rf)
p_4	r(B–H$_t$)(mean)	121.7(9)
p_5	r[B(1)–H(1,2)]	126.1(rf)
p_6	r[C(5)–H(5)]	112.3(4)
p_7	r[B(1)–H(1)] − r[B(2)–H(2)]	−0.9(f)
p_8	B(1)B(2)B(3)	54.3(5)
p_9	B(3)B(1)H(1,2)	112.1(4)
p_{10}	B(3)B(1)H(1)	66.6(49)
p_{11}	C(6)C(5)H(5)	110.6(30)
p_{12}	B(1)B(2)B(3)/B(1)B(4)B(3)	100.8(2)
p_{13}	r[B(2)–H(2)]/xy	45.7(19)
p_{14}	r[B(1)–H(1,2)]/xy	28.5(rf)
p_{15}	r[C(5)–H(5)]/xy	27.4(22)

[a] For definitions of parameters, see the text. [b] Figures in parentheses are the estimated standard deviations. Key: rf = refined then fixed; f = fixed.

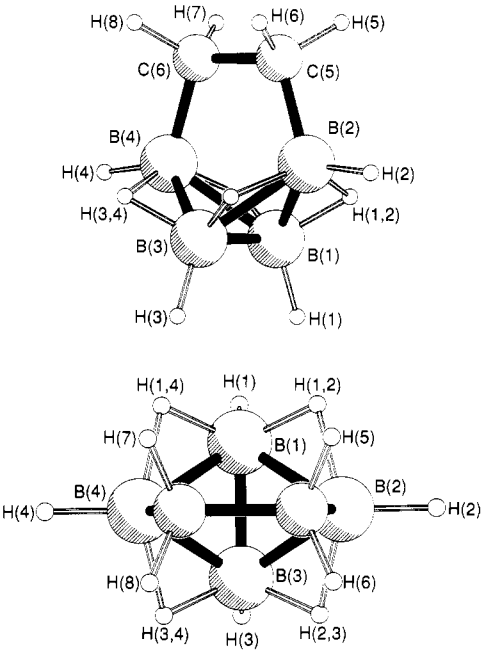

Figure 1. Views of the $B_4H_8(CH_2)_2$ molecule in the optimum refinement of the electron-diffraction data: (a, top) perspective view; (b, bottom) view showing the molecular C_{2v} symmetry.

(14) For example, see: (a) Hargittai, I., Hargittai, M., Eds.; *Stereochemical Applications of Gas-Phase Electron Diffraction, Part A*; VCH: Weinheim, Germany, 1990; p 301. (b) Hnyk, D.; Bühl, M.; Schleyer, P. v. R.; Volden, H. V.; Gundersen, S.; Müller, J.; Paetzold, P. *Inorg. Chem.* **1993**, *32*, 2442.
(15) Huntley, C. M.; Laurenson, G. S.; Rankin, D. W. H. *J. Chem. Soc., Dalton Trans.* **1980**, 954.
(16) Cradock, S.; Koprowski, J.; Rankin, D. W. H. *J. Mol. Struct.* **1981**, *77*, 113.
(17) Boyd, A. S. F.; Laurenson, G. S.; Rankin, D. W. H. *J. Mol. Struct.* **1981**, *71*, 217.
(18) Ross, A. W.; Fink, M.; Hilderbrandt, R. In *International Tables for Crystallography*; Wilson, A. J. C., Ed.; Kluwer Academic Publishers: Dordrecht, The Netherlands, Boston, MA, and London, 1992; Vol. C, p 245.
(19) See Hehre, W.; Radom, L.; Schleyer, P. v. R.; Pople, J. A. *Ab Initio Molecular Orbital Theory*; Wiley: New York, 1986.
(20) (a) Amos, W.; Rice, J. CADPAC, The Cambridge Analytical Derivatives Package, Issue 4.0. Cambridge, 1987. (b) Frisch, M. J.; Trucks, G. W.; Head-Gordon, M.; Gill, P. M. W.; Wong, M. W.; Foresman, J. B.; Schlegal, H. B.; Raghavachari, K.; Robb, M. A.; Replogle, E. S.; Gomperts, R.; Andres, J. L.; Binkley, J. S.; Gonzalez, C.; Martin, R.; Fox, D. J.; DeFrees, D. J.; Baker, J.; Stewart, J. J. P.; Pople, J. A. Gaussian Inc., Pittsburgh, PA, 1992.
(21) Huzinaga, S. *Approximate Atomic Wavefunctions*; University of Alberta: Edmonton, Canada, 1971.
(22) (a) Schleyer, P. v. R.; Gauss, J.; Bühl, M.; Greatrex, R.; Fox, M. A. *J. Chem. Soc., Chem. Commun.* **1993**, 1766. (b) Bühl, M.; Gauss, J.; Hofmann, M.; Schleyer, P. v. R. *J. Am. Chem. Soc.* **1993**, *115*, 12385.
(23) Brain, P. T.; Rankin, D. W. H.; Robertson, H. E.; Alberts, I. L.; Schleyer, P. v. R.; Hofmann, M. *Inorg. Chem.*, preceeding paper in this issue.
(24) See also: McKee, M. L. *J. Phys. Chem.* **1990**, *94*, 435.
(25) Gauss, J. *Chem. Phys. Lett.* **1992**, *191*, 614.

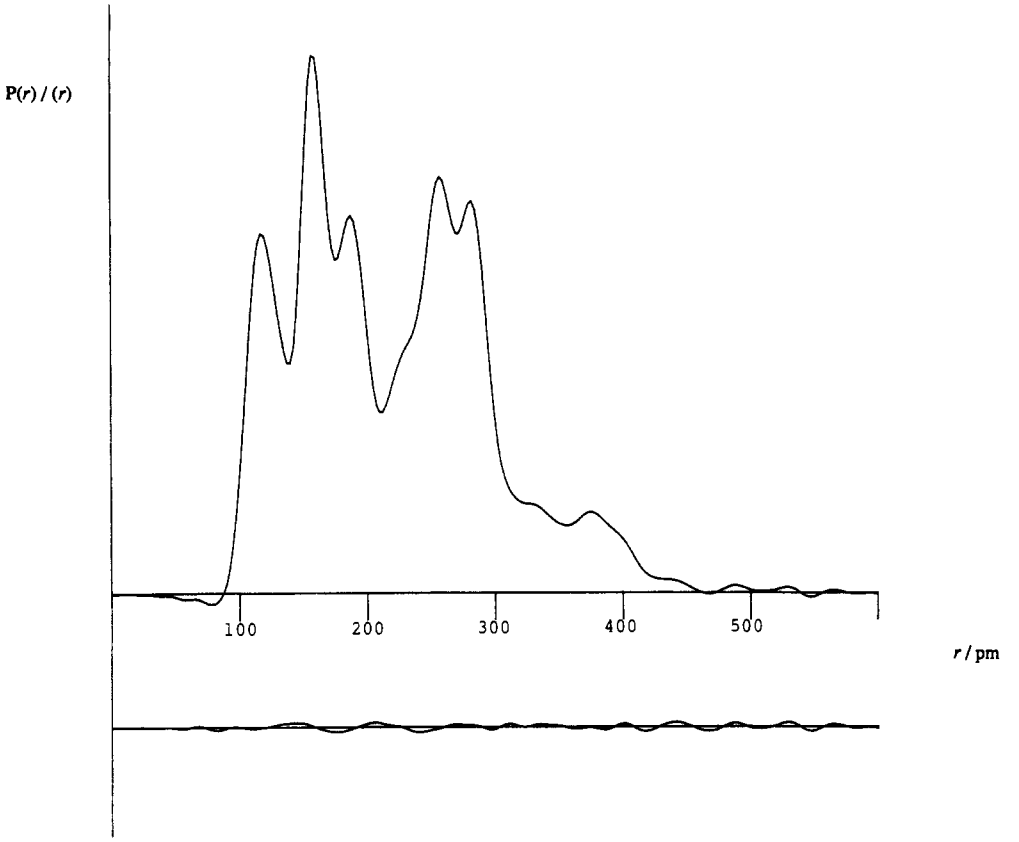

Figure 2. Observed and final weighted difference radial-distribution curves for $B_4H_8(CH_2)_2$. Before Fourier inversion the data were multiplied by $s \cdot \exp[(-0.00002s^2)/(Z_C - f_C)(Z_B - f_B)]$.

Table 3. Least-Squares Correlation Matrix (×100) for $B_4H_8(CH_2)_2$[a]

p_8	p_{10}	p_{11}	p_{13}	u_1	u_3	u_4	u_5	u_{12}	u_{15}	u_{19}	u_{20}	k_1	k_2	
78					68	-62								p_1
				74	-63	72		-54						p_2
60	58		-51		56							83	56	p_4
							70							p_6
	74		-50	-66	92	-89								p_8
	52													p_{12}
		-94							56		58			p_{15}
	-51				-69	86								u_1
				66										u_2
	66												55	u_3
	-61				-93									u_4
			-60						54					u_{10}
		-59											55	u_{15}
		-55							77					u_{18}
		-62								68				u_{20}
60	57		-60						55			54		k_2

[a] Only elements with absolute values >50 are shown. k is a scale factor.

basis (TZP for C and B; DZP for H).[26] The calculations were performed on the Convex C220 of the Institut für Organische Chemie der Universität Erlangen-Nürnberg and on a Cray YMP-8 of the Leibniz Rechenzentrum in Munich.

(26) Dunning, T. H. *J. Chem. Phys.* **1970**, *53*, 2823; **1971**, *55*, 716. The polarization functions were as follows: $d(B) = 0.386$, $d(C) = 0.654$, and $d(H) = 0.7$.

Molecular Model

On the basis of the NMR evidence and the *ab initio* calculations (see below), the molecular model used to generate the atomic coordinates of $B_4H_8(CH_2)_2$ was based on the structure established for tetraborane(10)[6] with the *endo* hydrogen atoms bonded to the "wing" boron atoms, B(2) and B(4), replaced by a bridging C_2H_4 unit. In the final refinements, such a model, with C_{2v}

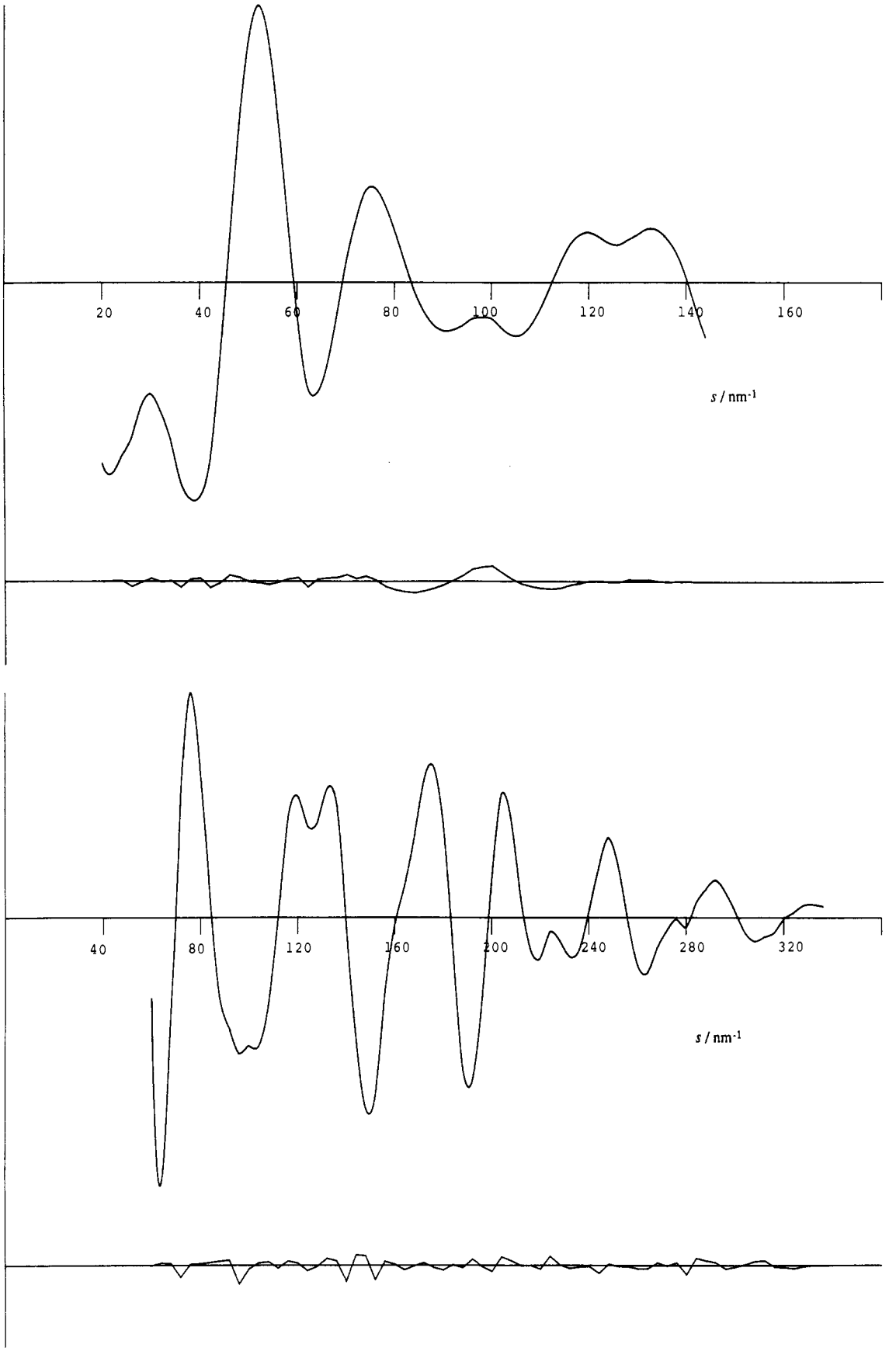

Figure 3. Observed and final weighted difference molecular-scattering intensity curves for $B_4H_8(CH_2)_2$. Nozzle-to-plate distances were (a, top) 286.1 and (b, bottom) 128.2 mm.

symmetry (the origin at the midpoint of B(1)–B(3) and the z axis parallel to the C_2 axis), was described by the 15 parameters listed in Table 2; the atom numbering scheme is shown in Figure 1.

The Heavy-Atom Skeleton. The B_4C_2 framework was described by five parameters; these consisted of the three bonded distances B(1)–B(2), B(2)–C(5), and C(5)–C(6), the angle B(1)B(2)B(3), and the dihedral angle between the planes B(1)B(2)B(3) and B(1)B(4)B(3), the so-called "butterfly" angle.

The Hydrogen Atoms. The four different types of hydrogen atom were defined by 10 refinable parameters. For the terminal hydrogen atoms attached to boron these consisted of a mean and difference of r[B(1)–H(1)] and r[B(2)–H(2)], p_4 and p_7, the angle B(3)B(1)H(1), and the elevation angle of the B(2)–H(2) bond below the *xy* plane (calculated for B(1)B(2)B(3)B(4) coplanar), p_{13}. A similar set of parameters was employed to define the positions of the bridging hydrogen atoms and those attached to carbon: (a) the bond lengths r[B(1)–H(1,2)] and r[C(5)–H(5)]; (b) the angles B(3)B(1)H(1,2) and C(6)C(5)H(5); (c) the elevation angles of the B(1)–H(1,2) and C(5)–H(5) bonds from the *xy* plane (calculated for B(1)B(2)B(3)B(4) coplanar), p_{14} and p_{15}, respectively.

Results

Refinement of the Structure. The radial-distribution curve for $B_4H_8(CH_2)_2$ shows five peaks at distances shorter than 300 pm; these occur near 119, 158, 186, 255, and 283 pm together with a shoulder at *ca.* 227 ppm (Figure 2). The peaks at $r < 200$ pm correspond to scattering from bonded atom pairs; the B–H (terminal and short bridging) and C–H bonds contribute to the peak at *ca.* 119 pm, while the peak at *ca.* 158 pm has contributions from the C–C, B–C, and long B–H_b bonded distances. The feature at *ca.* 186 pm represents scattering from the two types of B–B distances. The B(2)···B(4) and B(2)···C(6) nonbonded pairs contribute mainly to the peak at *ca.* 255 pm (together with some two-bond B···H and C···H distances) and the nonbonded pairs B(1)···C(5), C(5)···H(1,4), B(1)···H(2) and B(2)···H(1) are identified with the peak at *ca.* 283 pm. The shoulder at *ca.* 227 pm represents scattering from two-bond C···H and B···H atom pairs. The radial-distribution curve at $r > 300$ pm consists of several broad features encompassing the three-bond C···H and B···H nonbonded distances and scattering from the H···H nonbonded pairs in the molecule.

Of the 15 independent parameters defining the molecular geometry (Table 2), it was possible to refine all but four simultaneously. Each of the parameters p_3, p_5, and p_{14} was refined at some point in the analysis, but all were fixed in the final refinements due to the effects of correlation. The difference between the two types of B–H_t distances, p_7, could not be refined and was fixed at the value suggested by the *ab initio* study. In addition, it was possible to refine 12 amplitudes of vibration in the final refinements.

Molecular geometries possessing C_2 and C_s symmetry were also explored. In the former case this involved one additional parameter, p_{16}, allowing the C_2H_4 unit to twist about the C_2 axis out of the H(4)B(4)B(2)H(2) plane. Such refinements, using various starting values of p_{16} (e.g. 0°, 5°), always converged to a common minimum having p_{16} = 2.1(16)°, with negligible changes from the geometrical parameters and *R* factors obtained with the C_{2v} model. The small distortion angle is almost certainly a shrinkage effect. For the geometry with C_s symmetry, six additional parameters were required to define the differences between the B(1)–H(1,2)–B(2)–B(3) and B(1)–H(1,4)–B(4)–B(3) sections of the molecule. A large number of refinements were performed using these extra parameters, but in no case was significant deviation from C_{2v} symmetry observed.

The success of the final refinement, for which R_G = 0.069 (R_D = 0.058), may be assessed on the basis of the difference between the experimental and calculated radial-distribution curves (Figure 2). Figure 3 offers a similar comparison between the experimental and calculated molecular-scattering curves while the most significant elements of the least-squares correlation matrix are shown in Table 3. The structural details and vibrational amplitudes of the optimum refinement are listed in Table 4; Figure 1a affords a perspective view of the molecule.

The relatively low symmetry of the molecule $B_4H_8(CH_2)_2$, allied to the lack of any rigorously based vibrational assignment, ruled out the possibility of applying shrinkage corrections. However, there is no reason to suppose that such corrections would alter the results of the calculations significantly.

Table 4. Interatomic Distances (r_a/pm) and Amplitudes of Vibration (u/pm) for $B_4H_8(CH_2)_2$[a-c]

		distance	amplitude
r_1	B(1)–B(3)	172.9(17)	6.2(13)
r_2	B(1)–B(2)	189.5(3)	8.6(2)
r_3	C(5)–C(6)	156.8(rf)	4.9(10)
r_4	B(2)–C(5)	159.8(3)	6.4(10)
r_5	B(1)–H(1)	121.2(9)	
r_6	B(2)–H(2)	122.1(9)	9.7(4) (tied to u_5)
r_7	B(1)–H(1,2)	126.1(rf)	
r_8	B(2)–H(1,2)	145.2(13)	11.0(f)
r_9	C(5)–H(5)	112.3(4)	7.0(f)
r_{10}	B(2)···B(4)	259.8(4)	6.8(3) (tied to u_{10})
r_{11}	B(2)···C(6)	257.5(3)	
r_{12}	B(1)···C(5)	283.9(2)	8.3(2)
r_{13}	C···H (two bond)	223–241	9.6(8) (tied to u_{13})
r_{14}	B···H (two bond)	222–270	
r_{15}	C(5)···H(1,4)	298.7(3)	
r_{16}	B(1)···H(2)	282.1(23)	19.8(23) (tied to u_{15})
r_{17}	B(2)···H(1)	287.8(11)	
r_{18}	B···H (three bond)	331–333	18.1(17)
r_{19}	B,C···H (three bond)	368–382	12.5(10)
r_{20}	C(5)···H(1)	401.5(13)	14.9(19)

[a] For atom numbering scheme see Figure 1. Figures in parentheses are the estimated standard deviations. [b] H···H nonbonded distances were also included in the refinements, but are not listed here; amplitudes of vibration were fixed in the range 12–20 pm. [c] Key: rf = refined then fixed; f = fixed.

Table 5. *Ab Initio* Optimized Geometry (MP2/6-31G* level) for $B_4H_8(CH_2)_2$ (Distances in pm, Angles in deg)[a]

	MP2/6-31G*	electron diffraction[b]
	Distances	
B(1)–B(2)	185.9	189.5(3)
B(1)–B(3)	171.3	172.9(17)
B(2)–C(5)	160.4	159.8(3)
C(5)–C(6)	155.4	156.8(rf)
B(1)–H(1,2)	124.6	126.1(rf)
B(2)–H(1,2)	142.6	145.2(13)
B–H_t (mean)	119.2	121.7(9)
C(5)–H(5)	109.5	112.3(4)
	Angles	
B(1)B(2)B(3)	54.9	54.2(5)
B(1)B(2)B(3)/B(1)B(4)B(3) "butterfly"	101.1	100.8(2)

[a] For atom numbering scheme see Figure 1. [b] rf = refined then fixed. Values in parentheses are the estimated standard deviations.

***Ab Initio* and IGLO Calculations.** The structure of dimethylenetetraborane was optimized at the HF and MP2 levels of theory; the results for the latter are given in Table 5. The experimental (GED) and theoretical (MP2/6-316* level) geometries were used to calculate NMR chemical shifts for $B_4H_8(CH_2)_2$ using the IGLO method. The calculated values, DZ//MP2/6-31G* and DZ//GED, are given in Table 6 together with the experimental values.[4] The effect of electron correlation on the computed chemical shifts has been assessed using the GIAO-MP2 method.[25] With a few exceptions,[22a] computed ^{11}B chemical shifts are much less susceptible to electron-correlation effects.[22b]

At the Hartree–Fock level of theory, optimizations using 3-21G and 6-31G* basis sets gave a structure possessing C_s symmetry [B(2), B(4), and the C atoms in the mirror plane] at the potential-energy minimum; the C_{2v} geometry was observed to be a transition state at the HF/6-31G* level, one imaginary vibrational frequency being calculated, but only *ca.* 0.8 kJ mol^{-1} above the C_s minimum. However, reoptimization of this C_s form at the correlated MP2/6-31G* level resulted in the C_{2v} geometry being favored. No stationary point with either C_s or C_2 symmetry could be located at the MP2/6-31G* level. Thus, it appears that the C_{2v} structure

Table 6. IGLO Results for $B_4H_8(CH_2)_2$

level of theory//geometry	$\delta(^{11}B)$/ppm[a,b] B(2,4)	$\delta(^{11}B)$/ppm[a,b] B(1,3)	$\delta(^{13}C)$/ppm[b,c]	$\delta(^1H)$[b,c]/ppm H(1,3)	H(2,4)	H(bridge)	H(5–8)	rel energy[d,e]/kJ mol^{-1}
DZ//MP2/6-31G*	–0.1	–41.8	–2.2	2.1	3.7	–2.7	–0.7	0.0
II′//MP2/6-31G*	3.0	–39.0	–4.0	1.1	3.1	–2.6	–0.4	0.0
GIAO-MP2/TZP′//MP2/6-31G*	1.3	–42.4	1.7	1.6	3.3	–1.6	0.5	*f*
DZ//GED	3.0	–43.2	5.0	2.4	4.4	–2.2	0.4	30.5
GIAO-MP2/TZP′//GED	4.1	–43.6	9.2	1.9	4.1	–1.2	1.2	*f*
exptl	*3.2*	*–39.8*	*2.3*	*1.4*	*3.2*	*–1.0*	*0.6*	

[a] Relative to $BF_3{\cdot}OEt_2$. [b] See ref 4. [c] Relative to Me_4Si. [d] MP2/6-31G* single-point energy of the GED geometry relative to the MP2/6-31G* fully optimized geometry. [e] A partial optimization of the GED structure at the MP2/6-31G* level in which the heavy-atom skeleton remained fixed but the locations of the hydrogen atoms were permitted to vary gave a relative energy of 2.5 kJ mol^{-1}. [f] At the MP2/TZP′ level, the GED structure was found to be 45.2 kJ mol^{-1} higher in energy than the MP2/6-31G* fully optimized geometry.

Table 7. Geometrical Parameters for Tetraborane(10) and Its Adducts (Distances in pm, Angles in deg)[a,b]

Parameter	$B_4H_8(CH_2)_2$ GED[c]	$B_4H_8(CH_2)_2$ MP2[c]	B_4H_{10} GED[6]	B_4H_{10} MP2[8a]	*endo*-B_4H_8(CO) GED[7]	*endo*-B_4H_8(CO) MP2[8b]	*exo*-B_4H_8(CO) GED[7]	*exo*-B_4H_8(CO) MP2[8b]	*endo*-$B_4H_8{\cdot}PF_2(NMe_2)$ XRD[9]
"butterfly" angle at B(1)B(3)	100.8(2)	101.1	117.1(7)	117.3	134.9(38)	132.7	144.0(23)	140.8	137[d]
r[B(1)–B(2,4)]	189.5(3)	185.9	185.6(4)	183.5	184.9(4)	185.1	184.9(4)	181.5	184.4(11), 182.6(11)
r[B(1)–B(3)]	172.9(17)	171.3	170.5(12)	171.4	172.7(10)	169.9	172.7(10)	170.7	168.7(11)
r[B(3)–B(2,4)]	189.5(3)	185.9	185.6(4)	183.5	178.0(6)	178.0	178.0(6)	178.1	175.9(13), 175.3(14)
Δr(B–H_b)[e]	19.1(13)	18.0	16.9(13)	15.8	15.0(25)	5.8	15.0(25)	7.5	*f*

[a] GED = electron diffraction of the vapor; MP2 = theoretical optimization at the MP2/6-31G* level; XRD = X-ray diffraction of a single crystal. [b] Values in parentheses are the estimated standard deviations. [c] This work. [d] No esd reported. [e] $\Delta r(B–H_b) = r[B(2)–H(2,3)] - r[B(3)–H(2,3)]$. [f] Not accurately determined.

is a true minimum at the correlated level. Such calculations again demonstrate that it is essential to include the effects of electron correlation for such systems in order to obtain reliable theoretical geometries for comparison with experimental results.[8a,22]

At the MP2/6-31G*//MP2/6-31G* + ZPE(6-31G*, scaled) level, the association energy of B_4H_8 (C_1 symmetry) with C_2H_4 to form $B_4H_8(CH_2)_2$ is exothermic by 160.7 kJ mol^{-1} (*cf.* the corresponding association energy of B_4H_8 and CO, –95.3 kJ mol^{-1}).[8b] Thus, there is a considerable thermodynamic driving force for the formation of the title compound by the $B_4H_{10} + C_2H_4 \rightarrow B_4H_8(CH_2)_2 + H_2$ reaction, –96.5 kJ mol^{-1}, at the same level.

Discussion

The analysis of the electron-diffraction pattern of gaseous dimethylenetetraborane endorses the spectroscopic evidence[1-4] that the molecule consists of a C_{2v} geometry similar to that established for tetraborane(10)[6] in which the *endo* hydrogen atoms bonded to the "wing" boron atoms, B(2) and B(4), have been replaced by a bridging C_2H_4 unit.

The structural parameters derived by the *ab initio* computations (MP2/6-31G*) for $B_4H_8(CH_2)_2$ are in very good agreement with those refined from the electron-diffraction pattern (Table 5). Both geometries, GED and MP2, perform equally well in the IGLO ^{11}B chemical-shift calculations; employing the small DZ basis set, the deviation from the $\delta(^{11}B)$ experimental data[4] is *ca.* 2–3 ppm (see DZ//MP2/6-31G* and DZ//GED values in Table 6). At the highest uncorrelated level (II′//MP2/6-31G*), the agreement between computed and experimental $\delta(^{11}B)$ values is excellent (maximum deviation of less than 1 ppm). The performance of the computed ^{13}C chemical shifts is slightly worse; the II′//MP2/6-31G* value, –4.0 ppm, is too deshielded with respect to the experimental value of 2.3 ppm.[8a] The agreement at the correlated GIAO-MP2/TZP′//MP2/6-31G* level is slightly worse for the ^{11}B chemical shifts (maximum deviation 2.6 ppm) but improves considerably for the $\delta(^{13}C)$ value; 1.7 ppm *vs* the experimental value of 2.3 ppm. The agreement between the IGLO and experimental $\delta(^1H)$ values is satisfactory, with the largest deviation of 1.6 ppm found for the bridging hydrogens (Table 6).[8c]

In addition, single-point energy calculations at the MP2/6-31G* level have been performed for the electron-diffraction structure. Experimental borane and carborane geometries have been assessed previously by means of this "energy criterion".[8a,13] The experimental geometry is calculated to be 30.5 kJ mol^{-1} higher in energy than the fully optimized theoretical structure; a similar assessment at the somewhat higher MP2/TZP′ level gives a value of 45.2 kJ mol^{-1} (Table 6). Such an "excess energy" is found to be in the normal range for similarly large boranes and carbaboranes.[8a,13,23] A partial optimization of the electron-diffraction structure at the MP2/6-31G* level was also undertaken; the heavy-atom skeleton remained fixed but the locations of the hydrogen atoms were permitted to vary.[24] This so-called "hydrogen-relaxed" GED geometry of $B_4H_8(CH_2)_2$ optimized to a structure with a calculated energy only 2.5 kJ mol^{-1} greater than that for the fully optimized theoretical structure. Thus, the "excess energy" calculated for the GED structure is attributable almost completely to the positions of the hydrogen atoms.

Some structural parameters for tetraborane(10) and its adducts are presented in Table 7. It is noteworthy that, while the "hinge" B(1)–B(3) bond distance in $B_4H_8(CH_2)_2$ is observed to be very similar to those found for B_4H_{10}[6] and its carbonyl adducts,[7] the "hinge–wing" B(1)–B(2) bond distances are observed to be significantly longer (*ca.* 5 pm), and the "butterfly" angle at B(1)B(3) is very much more narrow than in any other compound in this class. Presumably, stabilization of the reactive intermediate $\{B_4H_8\}$, thought to be formed initially in the synthesis of $B_4H_8(CH_2)_2$, by interaction with ethene must require the closing of the "butterfly" B(1)B(3) angle relative to B_4H_{10}. The resulting compound, with a single C–C bond, undergoes attenuation of the B(1)–B(2) bond distances to alleviate the increased hydrogen atom nonbonded repulsions. This may also be reflected in the very marked asymmetry of the B–H_b distances which, compared to that in similar structures, is most pronounced for $B_4H_8(CH_2)_2$.

Finally, we note with interest the marked similarity between the structure of dimethylenetetraborane and the isoelectronic compound 3,4-bis(pentamethylcyclopentadienyl)tricyclo[3.1.0.0^{2,6}]-hexaphosphane, $P_6(C_5Me_5)_2$.[27] By analogy with $B_4H_8(CH_2)_2$, this may be regarded as a P_4 "butterfly" (the bicyclo[1.1.0]-tetraphospane structural element) bonded at the "wing" atoms, P(2) and P(5), to a $P_2(C_5Me)_5$ moiety. The "butterfly" is distorted very slightly from C_{2v} to C_2 symmetry; the "butterfly" angle at

(27) Jutzi, P.; Kroos, R., Müller, A.; Penk, M. *Angew. Chem., Int. Ed. Engl.* **1989**, *28*, 600.
(28) Brain, P. T.; Bühl, M.; Fox, M. A.; Greatrex, R.; Rankin, D. W. H.; Robertson, H. E.; Picton, M. J. Unpublished results.

ca. 115.5° is much wider than is found for the tetraborane derivative. In contrast to the C_2H_4 unit in $B_4H_8(CH_2)_2$, the $P_2(C_5Me_5)_2$ moiety is twisted by *ca.* 11° relative to the P(2)···P(5) (wing···wing) vector, presumably due to the steric demands of the pentamethylcyclopentadienyl groups. We are at present studying the gas-phase structures of $B_4H_8(CH_2)(CHMe)$ and $B_4H_8(CHMe)_2$ derivatives of the title compound, which also contain groups that may distort the heavy-atom skeleton.[28]

Acknowledgment. We thank the SERC for support of the Edinburgh Electron-Diffraction Service, including provision of microdensitometer facilities at the Daresbury laboratory and research fellowships for P.T.B., D.H., and H.E.R. We are indebted to Mr. N. K. Mooljee of the Edinburgh University Computing Service for technical assistance during the course of this work and to Mr. M. Hofmann of the Universität Erlangen-Nürnberg for performing the GIAO-MP2 calculations. M.K. was supported by a grant from the U.S. Army Research and Standardization Group (Europe). The work in Erlangen was supported by the Deutsche Forschungsgemeinschaft and the Fonds der Chemischen Industrie. We thank Prof. W. Kutzelnigg and Dr. M. Schindler for the Convex version of their IGLO program and Dr. J. Gauss for a copy of his GIAO-MP2 program.

Supplementary Material Available: A list of atomic coordinates for the GED and theoretically optimized geometries (1 page). Ordering information is given on any current masthead page.